Available online at www.sciencedirect.com

ScienceDirect

Geochimica et Cosmochimica Acta 220 (2018) 261–275

Geochimica et Cosmochimica Acta

www.elsevier.com/locate/gca

Calibrating amino acid $\delta^{13}C$ and $\delta^{15}N$ offsets between polyp and protein skeleton to develop proteinaceous deep-sea corals as paleoceanographic archives

Kelton W. McMahon [a,b,c,*], Branwen Williams [c], Thomas P. Guilderson [d,e], Danielle S. Glynn [d], Matthew D. McCarthy [d]

[a] *Graduate School of Oceanography, University of Rhode Island, Narragansett, RI 02882, USA*
[b] *Institute of Marine Sciences, University of California – Santa Cruz, Santa Cruz, CA 95064, USA*
[c] *W.M. Keck Science Department of Claremont McKenna College, Pitzer College, and Scripps College, Claremont, CA 91711, USA*
[d] *Ocean Sciences Department, University of California – Santa Cruz, Santa Cruz, CA 95064, USA*
[e] *Lawrence Livermore National Laboratory, Livermore, CA 94550, USA*

Received 29 August 2016; accepted in revised form 26 September 2017; Available online 9 October 2017

Abstract

Compound-specific stable isotopes of amino acids (CSI-AA) from proteinaceous deep-sea coral skeletons have the potential to improve paleoreconstructions of plankton community composition, and our understanding of the trophic dynamics and biogeochemical cycling of sinking organic matter in the Ocean. However, the assumption that the molecular isotopic values preserved in protein skeletal material reflect those of the living coral polyps has never been directly investigated in proteinaceous deep-sea corals. We examined CSI-AA from three genera of proteinaceous deep-sea corals from three oceanographically distinct regions of the North Pacific: *Primnoa* from the Gulf of Alaska, *Isidella* from the Central California Margin, and *Kulamanamana* from the North Pacific Subtropical Gyre. We found minimal offsets in the $\delta^{13}C$ values of both essential and non-essential AAs, and in the $\delta^{15}N$ values of source AAs, between paired samples of polyp tissue and protein skeleton. Using an essential AA $\delta^{13}C$ fingerprinting approach, we show that estimates of the relative contribution of eukaryotic microalgae and prokaryotic cyanobacteria to the sinking organic matter supporting deep-sea corals are the same when calculated from polyp tissue or recently deposited skeletal tissue. The $\delta^{15}N$ values of trophic AAs in skeletal tissue, on the other hand, were consistently 3–4‰ lower than polyp tissue for all three genera. We hypothesize that this offset reflects a partitioning of nitrogen flux through isotopic branch points in the synthesis of polyp (fast turnover tissue) and skeleton (slow, unidirectional incorporation). This offset indicates an underestimation, albeit correctable, of approximately half a trophic position from gorgonin protein-based deep-sea coral skeleton. Together, our observations open the door for applying many of the rapidly evolving CSI-AA based tools developed for metabolically active tissues in modern systems to archival coral tissues in a paleoceanographic context.

Keyword: Deep-sea coral; Compound-specific stable isotope analysis; Amino acid; Paleoceanography; Trophic dynamics; Biogeochemistry; Isotope fractionation

Abbreviations: AA, amino acid; CSI-AA, compound-specific stable isotopes of amino acids; SIA, stable isotope analysis; SIAR, stable isotope analysis in R; TP_{CSI-AA}, trophic position from compound-specific stable isotopes of amino acids

* Corresponding author at: Graduate School of Oceanography, University of Rhode Island, Narragansett, RI 02882, USA.
E-mail addresses: kelton_mcmahon@uri.edu (K.W. McMahon), bwilliams@keckscl.claremont.edu (B. Williams), guilderson1@llnl.gov (T.P. Guilderson), dglynn@ucsc.edu (D.S. Glynn), mdmccar@ucsc.edu (M.D. McCarthy).

https://doi.org/10.1016/j.gca.2017.09.048
0016-7037/

1. INTRODUCTION

A diverse array of analytical tools is used to examine ocean ecosystem and biogeochemistry cycling responses to changing climatic conditions (Gordon and Morel, 1983; Henderson, 2002; Rothwell and Rack, 2006; Katz et al., 2010). However, there is a critical gap in resolution between short-term, high-resolution instrumental records, such as remote satellite sensing, and most long-term, paleoceanographic sediment records. The geochemical composition of well preserved, accretionary biogenic tissues (hereafter bioarchives) has the potential to close this gap, shedding light on the structure and function of past ocean ecosystems and their responses to changing climatic and oceanographic conditions on the scale of decades to millennia (Druffel, 1997; Barker et al., 2005; Ehrlich, 2010; Robinson et al., 2014).

Deep-sea (azooxanthellate) corals were discovered over two hundred years ago (Roberts and Hirshfield, 2004), yet their potential as bioarchives of past ocean conditions is just starting to be fully appreciated (Robinson et al., 2014). They are found on hard substrates in every ocean from near the surface to over 6000 m water depth (Cairns, 2007). They provide a direct link to surface ocean processes by feeding opportunistically on recently exported surface-derived, sinking particulate organic matter (POM) (Ribes et al., 1999; Orejas et al., 2003; Roark et al., 2009). In the case of proteinaceous deep-sea corals, their skeletons are made of an extremely durable, cross-linked, fibrillar protein that is among the most diagenetically resistant proteinaceous materials known (Goldberg, 1974; Ehrlich, 2010; Strzepek et al., 2014). Proteinaceous skeletons are deposited in growth layers that are not metabolically reworked post-deposition (Roark et al., 2009; Sherwood and Edinger, 2009), and many species can live for hundreds to thousands of years (Roark et al., 2006, 2009; Guilderson et al., 2013). As such, proteinaceous deep-sea corals can be long-term (millennial), high-resolution (annual to decadal) bioarchives of past ocean conditions.

Much of the recent proxy development work with proteinaceous deep-sea corals has focused on stable isotope analysis (SIA) of total ("bulk") skeletal material, as a proxy for changes in surface ocean conditions (e.g., Heikoop et al., 2002; Sherwood et al., 2005, 2009; Williams et al., 2007; Hill et al., 2014). A main challenge to interpreting bulk stable isotope data in a paleo-context is determining whether changes in bulk stable isotope values are due to (1) changes in baseline dissolved inorganic carbon (^{13}DIC) or $^{15}NO_3$ values, (2) changes in plankton community composition, (3) changes in trophic dynamics of organic matter exported from the surface ocean (export production) or corals themselves, (4) changes in microbial reworking of sinking POM, or some combination of all of these factors (Wakeham and Lee, 1989; Meyers, 1994; Lehmann et al., 2002; Post, 2002). Compound-specific stable isotopes of individual amino acids (CSI-AA) offer a powerful suite of new tools to begin teasing apart these confounding variables (reviewed in Ohkouchi et al., 2017).

The potential of CSI-AA in paleoceanographic studies lies in the differential fractionation of individual AAs between diet and consumer. With respect to $\delta^{13}C$, there is a high degree of metabolic diversity in essential AA synthesis pathways among distinct lineages of primary producers (Hayes, 2001; Scott et al., 2006), which leads to unique essential AA $\delta^{13}C$ "fingerprints" of primary producers (Larsen et al., 2009, 2013; McMahon et al., 2011, 2015a, 2016). While the phylogenetic specificity of this approach is still coarse and will inherently be limited by the underlying diversity in central metabolism pathways among primary producers, our ability to identify primary producers at finer taxonomic scales using CSI-AA is improving (e.g., Larsen et al., 2009, 2013; McMahon et al., 2015a). These isotopic fingerprints are passed on to upper trophic level consumers, virtually unmodified, because animals acquire essential AAs directly from their diet (Reeds, 2000) with little to no isotopic fractionation between diet and consumer (Hare et al., 1991; Howland et al., 2003; McMahon et al., 2010). As a result, essential AA $\delta^{13}C$ fingerprinting tools are now rapidly developing, with the ultimate goal of quantifying the primary producer sources in food webs (e.g., Arthur et al., 2014; Nielsen and Winder, 2015; McMahon et al., 2016).

With respect to $\delta^{15}N$, individual AAs are commonly divided into trophic and source AAs (after Popp et al., 2007) based on their relative ^{15}N fractionation with trophic transfer ($\Delta^{15}N_{C\text{-}D}$) (reviewed in McMahon and McCarthy, 2016; Ohkouchi et al., 2017). Source AAs (e.g., phenylalanine: Phe) exhibit minimal nitrogen isotope fractionation during trophic transfer (McClelland and Montoya, 2002; Chikaraishi et al., 2009; McMahon et al., 2015b). Thus $\delta^{15}N_{Phe}$ has commonly been used as a proxy for the sources and cycling of nitrogen at the base of food webs ($\delta^{15}N_{baseline}$) (Décima et al., 2013; Sherwood et al., 2014; Vokhshoori and McCarthy, 2014; Lorrain et al., 2015). Trophic AAs (e.g., glutamic acid: Glu), on the other hand, undergo significant nitrogen isotope fractionation during transamination/deamination (McClelland and Montoya, 2002; Chikaraishi et al., 2009). When utilized together, the CSI-AA approach provides a metric of trophic position that is internally indexed to the $\delta^{15}N_{baseline}$ (Chikaraishi et al., 2007, 2009). It is important to note that the processes for AA $\delta^{15}N$ fractionation (degree of transamination/deamination; Braun et al., 2014) are largely independent from the processes for AA $\delta^{13}C$ fractionation (ability to synthesize carbon side chains; Hayes, 2001), providing complementary but distinct insight into the processing of organic matter.

In recent years, CSI-AA has increasingly been applied to proteinaceous deep-sea corals, with both AA $\delta^{13}C$ and $\delta^{15}N$ analyses used to understand shifting current systems on the Atlantic margin (Sherwood et al., 2011), changes in plankton community composition and nitrogen-fixation in the central Pacific (Sherwood et al., 2014; McMahon et al., 2015a), effects of long-term land use change on Gulf of Mexico N cycling (Prouty et al., 2014), and stability of mesophotic primary productivity in the western Pacific warm pool (Williams et al., 2016). However, a fundamental assumption for all such CSI-AA applications is that individual AA stable isotope values of bioarchival skeleton

material reflect the same AA isotope values in the metabolically active polyp tissue at the time of deposition. While AA stable isotope values have been well studied in metabolically active consumer tissues (reviewed in McMahon and McCarthy, 2016), these structural proteins typically have very different AA compositions and turnover rates (Ehrlich, 2010), which could potentially lead to differences in fractionation processes (e.g., Schmidt et al., 2004; Chikaraishi et al., 2014; Hebert et al., 2016). To our knowledge, this underlying question of AA $\delta^{13}C$ and $\delta^{15}N$ preservation in structural tissues of deep-sea corals has never been directly evaluated.

Here we present the first quantitative examination of individual AA stable isotope values ($\delta^{13}C$ and $\delta^{15}N$) in paired coral polyp tissue and recently deposited protein skeleton for three genera of deep-sea proteinaceous coral from three oceanographically distinct regions of the North Pacific (Fig. 1; Appendix A): Red Tree Coral *Primnoa pacifica* (Family: Primnoidae) from the Gulf of Alaska, Bamboo Coral *Isidella sp.* (Family: Isididae) from the California Current System, and Hawaiian Gold Coral *Kulamanamana haumeaae* (Family: Parazoanthidae) from the North Pacific Subtropical Gyre (NPSG), hereafter referred to as *Primnoa, Isidella,* and *Kulamanamana*, respectively. We tested the hypothesis that there would be no differences in individual AA $\delta^{13}C$ and $\delta^{15}N$ values between polyp tissue and recent skeletal material. We then tested whether metabolically active polyp tissue and proteinaceous skeleton produced the same results for two commonly used CSI-AA proxy approaches. First, we compared plankton community composition reconstructions from the paired tissue types using an AA $\delta^{13}C$ fingerprinting approach (e.g., McMahon et al., 2015a). Second, we reconstructed the trophic structure and baseline $\delta^{15}N$ values from both tissues, in corals spanning oligotrophic open ocean gyres to coastal eutrophic margins using AA $\delta^{15}N$ values (e.g., Sherwood et al., 2014).

2. METHODS

2.1. Study specimens and locations

2.1.1. Red Tree Coral: *Primnoa*

Primnoa pacifica (Cairns and Bayer, 2005) is an octocoral in the family Primnoidae that forms a large fan-shaped gross morphology comprised of a proteinaceous skeleton

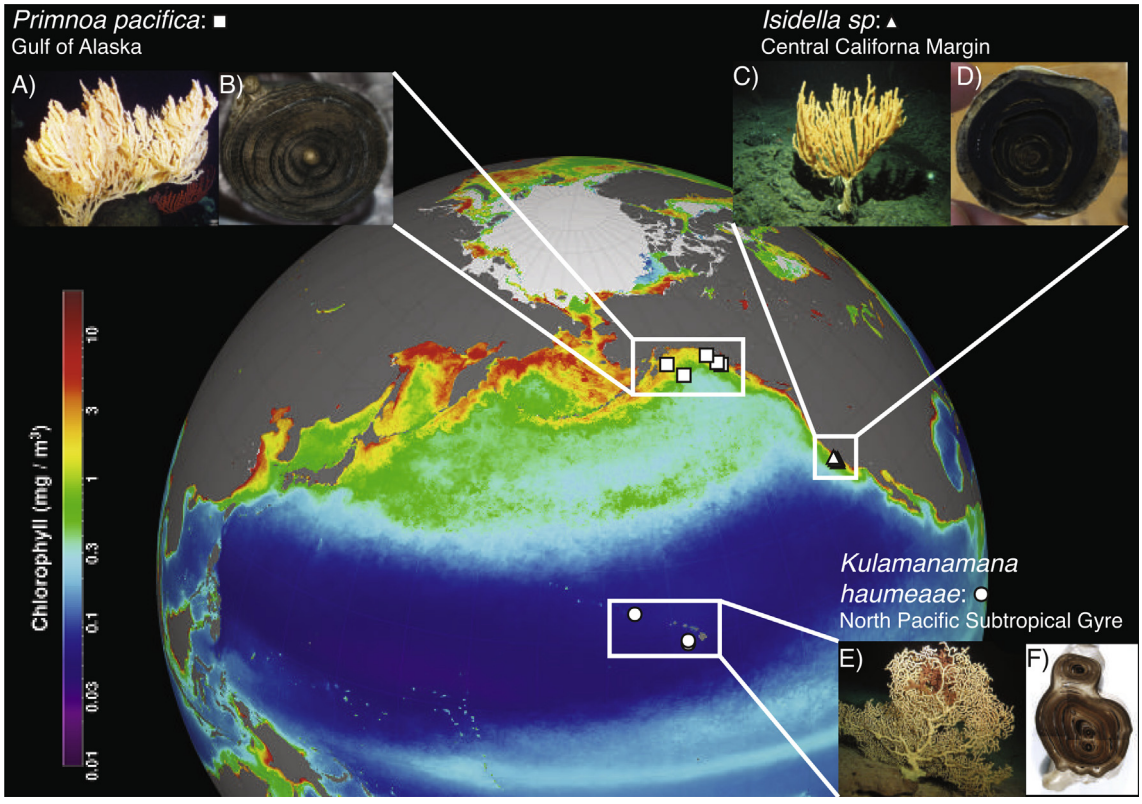

Fig. 1. Collection sites and deep-sea coral genera. Collection information for three genera of proteinaceous deep-sea coral, *Primnoa pacifica* (square symbols, $n = 5$) from the coastal region of the Gulf of Alaska, *Isidella* sp. (triangle symbols, $n = 5$) from Sur Ridge in the Central California Margin, and *Kulamanamana haumeaae* (circle symbols, $n = 3$) from the Hawaiian Archipelago in the North Pacific Subtropical Gyre. Color contours reflect remote sensing-derived chlorophyll a concentrations for the North Pacific from SeaWiFS seasonal climatology for the boreal spring 1998–2010 (image courtesy of Norman Kuring of the Ocean Biology Processing Group NASA/GSFC). Inset photos show the living coral structure and proteinaceous skeleton cross sections (enlarged Fig. A.1): (A) *Primnoa* colony (Photo credit: Ocean Networks Canada), (B) *Primnoa* cross-section (B. Williams Lab), (C) *Isidella* colony (NOAA Office of Ocean Exploration), (D) *Isidella* cross-section (M. McCarthy Lab), (E) *Kulamanamana* colony (Sinniger et al., 2013), and (F) *Kulamanama* cross-section (Sherwood et al., 2014). (For interpretation of the references to color in this figure legend, the reader is referred to the web version of this article.)

with radially alternating couplets of calcite and gorgonin material (Risk et al., 2002; Fig. A.1). These corals are slow growing, with radial growth rates of 100–300 μm yr^{-1} and lifespans of several hundred years (Andrews et al., 2002; Williams et al., 2007).

Here, five *Primnoa* specimens were collected from the Gulf of Alaska. Four live *Primnoa* were collected in 25–200 m water depth in the Gulf of Alaska in summer 2013, two using the H2000 ROV aboard the FSV Alaska Provider from Scripps University and two via bottom trawl. One dead specimen was collected from an unknown depth via bottom trawl in summer 2010 (Fig. 1; Table A.1). The coastal regions of the Gulf of Alaska are iron-rich, sourced from cross-shelf exchange and vertical mixing (Bruland et al., 2001; Childers et al., 2005; Ladd et al., 2005), which support high primary productivity characterized by diatoms and flagellates (Sambrotto and Lorenzen, 1986; Strom et al., 2006). In deeper water (400 m), $\delta^{15}N$ value of the nitrate is 4–5‰ (Wu et al., 1997). There is a strong seasonal cycle in nitrogen dynamics in the coastal region reflecting the supply of nutrients to the surface waters via upwelling during the early summer followed by rapid nutrient drawdown by summer phytoplankton blooms as the summer progresses and upwelling stops (Wu et al., 1997).

2.1.2. Bamboo coral: Isidella

Isidella sp. (Gray, 1857) is an octocoral in the family Isididae that forms a skeleton of high magnesium calcite internodes several centimeters long interspersed by proteinaceous gorgonin organic nodes (4–25 mm long) (Fig. A.1). These coral grow in candelabra-like shapes to heights greater than 2 m (Fig. A.1). They are slow growing (radial growth rates of 50–150 μm yr^{-1}), with lifespans reaching several hundred years (Thresher et al., 2004; Roark et al., 2005).

Here, five live specimens of the genus *Isidella* were collected in 1125–1250 m water depth from the California Margin (Sur Ridge) offshore of central California using the Monterey Bay Area Research Institute (MBARI) ROV Doc Ricketts in the summer of 2014 (Fig. 1; Table A.1). The California Margin is one of the most productive zones of the World Ocean, with strong seasonal coastal upwelling from April through early winter (Strub et al., 1987; García-Reyes and Largier, 2012) generating a nutrient-rich environment supporting substantial productivity (Bruland et al., 2001). Sur Ridge in the Central California Margin is a high nutrient and low chlorophyll (HNLC) zone (Hutchins and Bruland, 1998; Walker and McCarthy, 2012). The southward-flowing California Current bathes this region with NO_3^- of oceanic origin, while the northward-flowing California Undercurrent and the weaker nearshore Davidson Current entrain ^{15}N-enriched NO_3^- associated with enhanced denitrification from the high productivity, low oxygen Eastern Tropical North Pacific (Altabet et al., 1999; Voss et al., 2001; Collins et al., 2003).

2.1.3. Hawaiian Gold Coral: Kulamanamana

Kulamanamana haumeaae (Sinniger et al., 2013) is a parasitic zoantharian in the family Parazoanthidae that secretes a scleroprotein skeleton that covers and eventually extends beyond its host coral colony. This coral forms a sea fan shape with heights of several meters (Parrish, 2015; Fig. A.1). It is a very long-lived, slow growing coral, with lifespans of thousands of years and radial growth rates of 25–100 μm yr^{-1} (Roark et al., 2006, 2009; Guilderson et al., 2013).

Here, three live *Kulamanamana* colonies were collected in 350–410 m water depth from seamounts in the Hawaiian Archipelago using the HURL/NOAA Pisces V submersible in the summer of 2004 and 2007 (Fig. 1; Table A.1) (Guilderson et al., 2013). The NPSG is characterized by exceedingly low dissolved nutrients (<10 nmol NO_3^- in the mixed layer) and is dominated by small cell prokaryotic cyanobacterial production (Karl et al., 2001). The nitrogen balance and controls on new production in this system are not strictly limited by available fixed nitrogen (Eppley et al., 1977), and there is significant nitrogen fixation with characteristically low $\delta^{15}N$ values (Karl et al., 2008; Church et al., 2009).

2.2. Sample preparation and analysis

2.2.1. Sample Preparation

All coral colonies were rinsed with saltwater followed by distilled water and air-dried prior to being transferred to onshore laboratories. Encrusted polyp tissue was then peeled as a single mass from the skeleton of each coral colony with forceps and dried again at 50 °C for 24 h. After drying, the polyp tissue was homogenized, reflecting a colony wide composite sample. Deep-sea coral polyp tissues are very lipid rich (Hamoutene et al., 2008), and therefore polyp tissue samples were lipid extracted three times following the conventional methanol/chloroform protocol of Bligh and Dyer (1959) prior to analysis of CSI-AA to improve chromatography. The proteinaceous nodes of *Isidella* were separated from the carbonate internodes with a scalpel according to Schiff et al. (2014). Both *Primnoa* and *Kulamanamana* skeletons were sectioned at the base and polished according to Sherwood et al. (2014). The outermost edge of the protein skeleton (~200 μm radial depth, 5–7 mm band parallel to the growth axis) from all three coral genera was sampled with a computerized Merchantek micromill. Skeleton samples were individually acid washed in 1 N HCl in glass vials for four hours, rinsed three times in Milli-Q water, and dried overnight at 50 °C to remove calcium carbonate prior to analysis of CSI-AA to improve chromatography.

2.2.2. Stable isotope analysis

Bulk $\delta^{13}C$ and $\delta^{15}N$ values and elemental ratios for coral skeleton material as well as coral polyp material before and after lipid extraction (Appendix B; Table B.1) were conducted at the University of California – Santa Cruz using standard protocols of the Stable Isotope Laboratory (http://emerald.ucsc.edu/~silab/). Isotope values were corrected using an internal laboratory acetanilide standard, and in turn referenced to international IAEA standards. More detailed descriptions of coral tissue bulk analyses and data interpretation are given in Appendix B.

CSI-AA was conducted on polyp tissue and proteinaceous skeleton using 3 mg for $\delta^{13}C$ and 6 mg for $\delta^{15}N$. Samples were acid hydrolyzed in 1 ml of 6 N HCl at 110 °C for 20 h to isolate the total free AAs and then evaporated to dryness under a gentle stream of ultra-high purity N_2. All samples were redissolved in 0.01 N HCl and passed through 0.45 μm Millipore glass-fiber filters followed by rinses with additional 0.01 N HCl. Samples were then passed through individual cation exchange columns (Dowex 50WX* 400 ion exchange resin), rinsed with 0.01 N HCl, and eluted into muffled glassware with 2 N ammonia hydroxide. Dried samples were derivatized by esterification with acidified iso-propanol followed by acylation with trifluoroacetic anhydride (Silfer et al., 1991). Derivatized samples were extracted with P-buffer ($KH_2PO_4 + Na_2HPO_4$ in Milli-Q water, pH 7) and chloroform three times with centrifugation (600 g) and organic phase extraction between each round (Ueda et al., 1989). Samples were evaporated to dryness under a gentle stream of ultra-high purity N_2 prior to neutralization with 2 N HCl at 110 °C for 5 min. Dried samples were acylated once again and then brought up in ethyl acetate for CSI-AA analysis.

For AA $\delta^{13}C$ analyses, the derivatized AAs were injected in split mode at 250 °C and separated on a DB-5 column (50 m × 0.5 mm inner diameter; 0.25 μm film thickness; Agilent Technologies, Santa Clara, California, USA) in a Thermo Trace Ultra gas chromatograph (GC) at the University of California – Santa Cruz. The separated AA peaks were analyzed on a Finnegan MAT Delta^{Plus} XL isotope ratio mass spectrometer (IRMS) interfaced to the GC through a GC-C III combustion furnace (960 °C) and reduction furnace (630 °C). For AA $\delta^{15}N$ analyses, the derivatized AAs were injected in splitless mode at 250 °C and separated on a BPX5 column (60 m × 0.32 mm inner diameter, 1.0 μm film thickness; SGE Analytical Science, Austin, Texas, USA) in the same CG-C-IRMS interfaced through a combustion furnace (980 °C), reduction furnace (650 °C), and a liquid nitrogen trap.

For carbon, we assigned glutamic acid (Glu), aspartic acid (Asp), alanine (Ala), proline (Pro), glycine (Gly), and serine (Ser) as non-essential AAs, and threonine (Thr), leucine (Leu), isoleucine (Ile), valine (Val), and phenylalanine (Phe) as essential AAs (Reeds, 2000). For nitrogen, we assigned Glu, Asp, Ala, Leu, Ile, Pro, Val as trophic AAs, and Phe, Methionine (Met), and Lysine (Lys) as source AAs (Popp et al., 2007). Gly, Ser, and Thr were kept as separate groups given the lack of consensus on degree of trophic fractionation between diet and consumer (reviewed in McMahon and McCarthy, 2016). It should be noted that acid hydrolysis converts glutamine (Gln) and aspartamine (Asn) into Glu and Asp, respectively, due to cleavage of the terminal amine group, resulting in the measurement of combined Gln + Glu (referred to hereby as Glu), and Asn +Asp (referred to hereby as Asp).

Standardization of runs was achieved using intermittent pulses of a CO_2 or N_2 reference gas of known isotopic value and internal nor-Leucine standards. All CSI-AA samples were analyzed in triplicate along with AA standards of known isotopic composition (Sigma–Aldrich Co.). The variability reported for $\delta^{13}C$ and $\delta^{15}N$ value of each AA measured (Tables C.1–C.4) therefore represents the analytical variation for $n = 3$ replicate GC-C-IRMS measurements. The long-term reproducibility of stable isotope values in a laboratory algal standard provides an estimate of full protocol reproducibility (replicate hydrolysis, wet chemistry, and analysis): $\delta^{13}C = \pm 0.7‰$ and $\delta^{15}N = \pm 0.3‰$ (calculated as the long-term SD across >100 separate full analyses, averaged across all individual AAs).

2.3. Data analysis

We used principal component analysis to visualize multivariate patterns in the $\delta^{13}C$ values of individual AAs (Ala, Asp, Gly, Glu, Ile, Leu, Phe, Pro, Ser, Thr, Val) in polyp tissue and skeleton of the three deep-sea coral genera (Appendix C, Table C.5). Individual AA stable isotope offsets were calculated as the difference in isotope value ($\delta^{13}C$ or $\delta^{15}N$) between paired polyp and skeleton samples for each individual from the three genera of deep-sea coral. We used separate one-sample *t*-tests to determine if individual AA $\delta^{13}C$ and $\delta^{15}N$ offsets between polyp and skeleton were significantly different from zero ($\alpha = 0.05$). For all statistical analyses $n = 5$ individuals for *Primnoa* and *Isidella* and $n = 3$ individuals for *Kulamamanama*. All data conformed to the assumptions of their respective statistical tests.

We used an AA isotope fingerprinting approach to examine the composition of primary producers fueling export production to deep-sea corals in each of the three study regions: Gulf of Alaska (*Primnoa*), Central California Margin (*Isidella*), and NPSG (*Kulamanamana*) (sensu McMahon et al., 2015a; see Appendix C for details). Briefly, we calculated the relative contribution of key plankton end members (eukaryotic microalgae, prokaryotic cyanobacteria, and heterotrophic bacteria) contributing carbon to each coral colony via export production in a fully Bayesian stable isotope mixing framework (Parnell et al., 2010; Ward et al., 2010) within the Stable Isotope Analysis in R (SIAR) package (R Core Team, 2013). We used published essential AA $\delta^{13}C$ data (Thr, Ile, Val, Phe, and Leu) from eukaryotic microalgae, cyanobacteria, and heterotrophic bacteria (Larsen et al., 2009, 2013; Lehman, 2009) as the source data set for the mixing model (Table C.6). We used normalized essential AA $\delta^{13}C$ values of end members and coral tissues (polyp and skeleton) to facilitate comparisons of the AA $\delta^{13}C$ fingerprints across different regions and growing conditions (see Appendix C for justification). To do this, we subtracted the mean of all five essential AA $\delta^{13}C$ values from each individual essential AA $\delta^{13}C$ value for each sample (sensu Larsen et al., 2015). In SIAR, we ran 500,000 iterations with an initial discard of the first 50,000 iterations as burn-in. We used separate One-Way Analyses of Variance (ANOVA) with Tukey's Honestly Significant Difference (HSD) post hoc tests ($\alpha = 0.05$) to look for differences in relative contribution of each end member among the three coral genera. We used separate one-sample *t*-tests to see if the differences in the relative contribution of potential end members calculated from coral polyp tissue vs. skeleton were significantly different from 0 ($\alpha = 0.05$).

We examined the differences in mean trophic AA $\delta^{15}N$ offsets (calculated as the mean $\delta^{15}N$ offset between polyp and skeleton averaged across all trophic AAs for each coral) among the three genera of coral using a One-Way ANVOA and Tukey's HSD post hoc test ($\alpha = 0.05$). We calculated separate $TP_{CSI\text{-}AA}$ values of deep-sea corals based on the AA $\delta^{15}N$ values from polyp tissue and skeleton using the single $TDF_{Glu\text{-}Phe}$ approach of Chikaraishi et al. (2009):

$$TP_{CSI-AA-single\ TDF} = 1 + \left[\frac{\delta^{15}N_{Glu} - \delta^{15}N_{Phe} - \beta}{TDF_{Glu-Phe}}\right] \quad (1)$$

where $\delta^{15}N_{Glu}$ and $\delta^{15}N_{Phe}$ represent the stable nitrogen isotope values of coral Glu and Phe, respectively, β represents the difference in $\delta^{15}N$ between Glu and Phe of primary producers (3.4‰ for aquatic cyanobacteria and algae (McClelland and Montoya, 2002; Chikaraishi et al., 2010)), and $TDF_{Glu\text{-}Phe}$ is the literature trophic discrimination factor value of 7.6‰ (Chikaraishi et al., 2009). We then used separate one-sample *t*-tests to see if the differences in $TP_{CSI\text{-}AA}$ offsets calculated from coral polyp tissue vs. skeleton were significantly different from 0 ($\alpha = 0.05$). All statistics were performed in R version 3.0.2 using RStudio interface version 0.98.501 (R Core Team, 2013).

3. RESULTS

3.1. Bulk elemental and isotopic composition

Detailed analysis of bulk isotopic and elemental composition for coral skeleton and polyp material is given in Appendix B. The $\delta^{13}C$ values for coral skeleton material (-15.9 ± 0.9‰) was ~3.5‰ more enriched than lipid-intact polyp material (-19.4 ± 1.0‰), though both tissues had consistent $\delta^{13}C$ values across all three genera examined (Table B.1). The $\delta^{13}C$ values of lipid extracted polyp material (-15.5 ± 0.7‰) were 4‰ lower than lipid-intact polyps and very similar to corresponding skeleton material (mean offset -0.4 ± 0.5‰) (Table B.1). Lipid extraction also altered polyp tissue C/N ratios. Lipid-extracted polyp tissues had much lower C/N ratios (3.1 ± 0.3) than lipid-intact polyps (4.8 ± 0.7) and were very similar to coral proteinaceous skeleton (2.9 ± 0.3). Much like $\delta^{13}C$ values, C/N ratios were consistent across all three genera examined. In contrast, the $\delta^{15}N$ values were more variable among the three genera for both skeleton (mean 13.8 ± 1.0‰ for *Primnoa*; 16.0 ± 0.7‰ for *Isadella*, and 10.3 ± 0.3‰ for *Kulamanamana*) and lipid-intact polyp tissue (mean 11.2 ± 0.4‰ for *Primnoa*; 14.8 ± 0.6‰ for *Isadella*, and 8.3 ± 0.3‰ for *Kulamanamana*) (Table B.1). On average, coral polyp tissue was 1.9 ± 0.8‰ more enriched in ^{15}N than coral skeleton (Table B.1).

3.2. Amino acid carbon isotopes

Individual AA $\delta^{13}C$ values differed significantly among the three coral genera (Fig. 2), with *Primnoa* from the Gulf of Alaska and *Isidella* from the Sur Ridge generally having more positive AA $\delta^{13}C$ values than *Kulamanamana* from the NPSG. Given the substantially larger differences in individual AA $\delta^{13}C$ values among different coral genera compared to among individuals within a genus, all three corals were separated in multivariate space based on

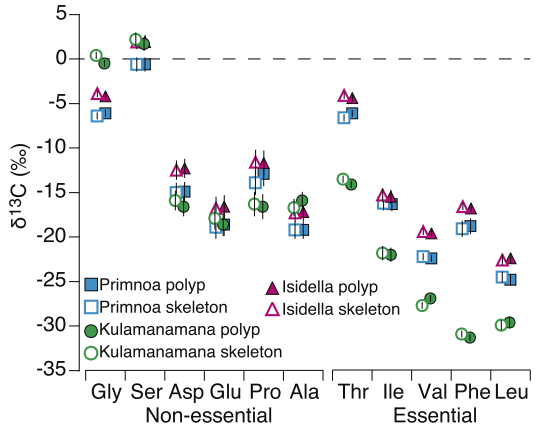

Fig. 2. Coral amino acid $\delta^{13}C$ values. Mean individual amino acid $\delta^{13}C$ values (‰ ±SD) in polyp tissue (filled symbols) and proteinaceous skeleton (open symbols) from three genera of proteinaceous deep-sea coral: *Primnoa pacifica* (cyan squares, $n = 5$), *Isidella* sp. (magenta triangles, $n = 5$), and *Kulamanamana haumeaae* (green circles, $n = 3$). (For interpretation of the references to color in this figure legend, the reader is referred to the web version of this article.)

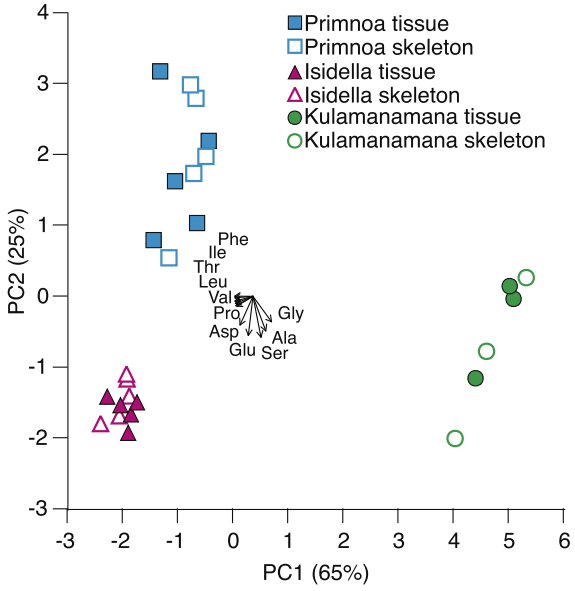

Fig. 3. Principal component analysis of eleven coral amino acid $\delta^{13}C$ values from polyp tissues (filled symbols) and proteinaceous skeleton (open symbols) of three genera of deep-sea corals: *Primnoa pacifica* ($n = 5$ individual colonies) from the Gulf of Alaska, *Isidella* sp. ($n = 5$ individual colonies) from the Central California Margin, and *Kulamanamana haumeaae* ($n = 3$ individual colonies) from the North Pacific Subtropical Gyre. Variance of principal components is in parentheses on each axis (Table C.5). Loadings of the eleven amino acids (conventional three-letter abbreviation format) are shown as arrows from the center (Table C.5).

principal component analysis of all eleven AA $\delta^{13}C$ values (Fig. 3, Table C.5).

There was little to no variation in individual AA $\delta^{13}C$ values between skeleton and polyp tissue within an individual: mean $\delta^{13}C$ offset was -0.2 ± 0.4‰ for *Primnoa*, 0.0 ± 0.2‰ for *Isidella* and 0.2 ± 0.6‰ for *Kulamamana* (calculated as the average offset for all AAs analyzed, averaged across all individuals within a genus; Fig. 4). No individual AA $\delta^{13}C$ offsets between skeleton and polyp tissue were greater than 1‰, and only the non-essential AA Pro in *Primnoa* had a $\delta^{13}C$ offset that was significantly different from 0‰ (-1.0 ± 0.7‰; Table 1). As a result, the skeleton and polyp tissue from a single genus always clustered together in multivariate space (Fig. 3, Table C.5).

Using an AA isotope fingerprinting approach in a Bayesian stable isotope mixing model, we compared estimates of the relative contribution of eukaryotic microalgae and prokaryotic cyanobacteria to corals calculated from both coral skeleton and polyp tissue. The relative contribution results were very similar regardless of tissue type (Fig. 5). The mean absolute value difference in relative contribution calculated from polyp vs. skeleton was $6 \pm 3\%$ for *Primnoa*, $4 \pm 2\%$ for *Isidella*, and $5 \pm 2\%$ for *Kulamanamana* (calculated as the absolute value of the difference in relative contribution for each end member between polyp tissue and skeleton, averaged across all three end members for all individuals within a coral genera). This 4–6% variability between tissue types was within the variance in model output after 500,000 iterations of the SIAR mixing model ($8 \pm 1\%$).

We did find significant differences in the relative contribution of cyanobacteria-derived carbon (One-way ANOVA, $F_{2,10} = 235.5$, $p = 3.9e^{-9}$) and eukaryotic microalgae-derived carbon (One-way ANOVA, $F_{2,10} = 410.5$, $p = 2.5e^{-10}$) among the three corals (calculated from polyp tissue, but the results were the same for skeleton). Both *Primnoa* from the Gulf of Alaska ($77 \pm 2\%$) and *Isidella* from the Central California Margin ($68 \pm 4\%$) relied heavily on export production fueled by eukaryotic microalgae (Tukey's HSD, $p < 0.05$) (Fig. 5). Conversely, *Kulamanamana* from the NPSG received relatively little input from eukaryotic microalgae ($9 \pm 5\%$) (Tukey's HSD, $p < 0.05$), instead receiving the majority of its carbon from cyanobacteria-fixed carbon ($74 \pm 1\%$) (Tukey's HSD, $p < 0.05$) (Fig. 5). All three corals showed a small and relatively consistent contribution of carbon from heterotrophic bacteria ($12 \pm 4\%$ averaged across all three genera) (Fig. 5).

3.3. Amino acid nitrogen isotopes

As with carbon, individual AA $\delta^{15}N$ values differed significantly among the three coral genera (Fig. 6), with *Isidella* from the California Margin having the highest AA $\delta^{15}N$ values and *Kulamanamana* from the NPSG having the lowest AA $\delta^{15}N$ values. The trophic AAs were more positive than the source AAs, and Thr had the characteristically most negative $\delta^{15}N$ values.

$\delta^{15}N$ values did not differ significantly between coral skeleton and polyp tissue for any of the measurable source AAs: Phe (mean offset across all three genera $= -0.1 \pm$ 0.1‰), Lys (0.3 ± 0.1‰), and Met (0.1‰; however, Met was only present in sufficient quantity for analysis in *Primnoa*) (Fig. 7; Table 1). However, the mean offset in trophic AA $\delta^{15}N$ values between skeleton and polyp were significantly greater than 0‰ for all three genera: *Primnoa* $= -2.8 \pm 0.2$‰ (one sample *t*-test, $t_4 = -32.4$, $p = 5.4e^{-6}$), *Isidella* $= -3.5 \pm 0.4$‰ (one sample *t*-test, $t_4 = -22.0$, $p = 2.5e^{-5}$), and *Kulamanamana* $= -3.2 \pm 0.1$‰ (one sample *t*-test, $t_2 = -56.8$, $p = 3.1e^{-4}$) (averaged across all trophic AAs within an individual and then averaged across all individuals within a genus) (Fig. 7). In particular, the mean offset for the canonical trophic AA Glu was remarkably consistent across all three coral genera: *Primnoa* $= -3.4 \pm 0.5$‰, *Isidella* $= -3.4 \pm 0.5$‰, and *Kulamanamana* $= -3.4 \pm 0.2$‰ (averaged across individuals within a genus) (Fig. 7, Table 1). Thr $\delta^{15}N$ values were consistently offset between skeleton and polyp tissue for all three genera (mean offset across all three genera $= 2.8 \pm 0.6$‰), but in the opposite direction as the trophic AAs (Fig. 7, Table 1). Gly and Ser had variable $\delta^{15}N$ offsets among the three genera though they were always closer to 0‰ than the trophic AAs and Thr (Fig. 7, Table 1).

All three coral genera had similar $TP_{CSI\text{-}AA}$ values when calculated from polyp tissue: *Primnoa* $= 2.4 \pm 0.2$, *Isidella* $= 2.4 \pm 0.1$, and *Kulamanamana* $= 2.6 \pm 0.1$ (averaged across individuals within a genus). However, given the large -3.4‰ offset in $\delta^{15}N$ value of Glu between skeleton and polyp tissue, coincident with no appreciable offset in Phe $\delta^{15}N$ value, $TP_{CSI\text{-}AA}$ estimates were nearly half a trophic level lower when calculated from skeleton AA $\delta^{15}N$ data, compared to estimates from polyp data. The mean $TP_{CSI\text{-}AA}$ offsets between skeleton and polyp were very similar among genera: for *Primnoa* $= -0.4 \pm 0.1$ (one sample *t*-test, $t_4 = -15.7$, $p = 9.5e^{-5}$), *Isidella* $= -0.4 \pm 0.1$

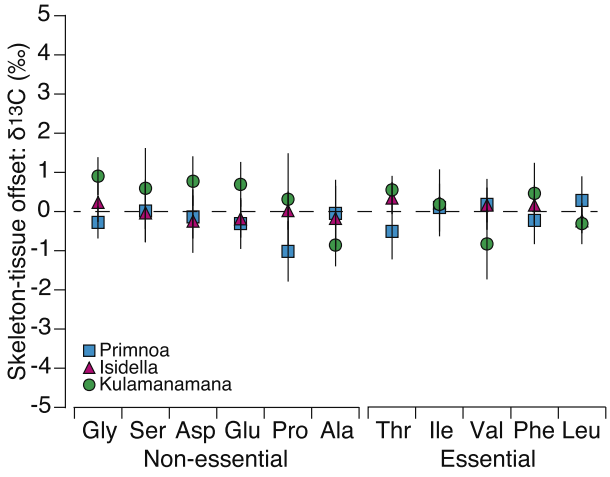

Fig. 4. Coral amino acid $\delta^{13}C$ offsets between tissues. Mean (‰ ±SD) individual amino acid $\delta^{13}C$ offset (skeleton minus polyp tissue) from three genera of proteinaceous deep-sea coral: *Primnoa pacifica* (cyan squares, $n = 5$), *Isidella* sp. (magenta triangles, $n = 5$), and *Kulamanamana haumeaae* (green circles, $n = 3$). (For interpretation of the references to color in this figure legend, the reader is referred to the web version of this article.)

Table 1
Mean (‰ ±SD) offset (skeleton minus polyp tissue) of individual amino acid $\delta^{13}C$ and $\delta^{15}N$ values for three genera of proteinaceous deep-sea coral. One sample *t*-tests determined if mean offsets were significantly different from 0‰ (*t* statistic [df = 4 for *Primnoa* and *Isidella*, df = 2 for *Kulamanamana*] $^{ns}p > 0.05$, $^{*}p < 0.05$, $^{**}p < 0.01$, $^{***}p < 0.001$). Amino acid names are in conventional three-letter abbreviation format. Essential and non-essential amino acids designated with ^{E} and ^{N}, respectively; trophic and source amino acids designated with ^{T} and ^{S}, respectively; amino acids with poorly characterized fractionation during trophic transfer designated with $^{?}$. na = not analyzed.

	Primnoa pacifica		*Isidella* sp.		*Kulamanamana haumeaae*	
	$\delta^{13}C$ (‰)	$\delta^{15}N$ (‰)	$\delta^{13}C$ (‰)	$\delta^{15}N$ (‰)	$\delta^{13}C$ (‰)	$\delta^{15}N$ (‰)
$Ala^{N,T}$	-0.1 ± 0.8 (-0.13^{ns})	-3.1 ± 0.5 (-15.42^{***})	-0.2 ± 0.8 (-0.49^{ns})	-3.8 ± 0.7 (-12.90^{***})	-0.9 ± 0.5 (-2.90^{ns})	-3.4 ± 0.4 (-13.78^{**})
$Asp^{N,T}$	-0.1 ± 0.5 (-0.59^{ns})	-3.2 ± 0.3 (-20.53^{***})	-0.2 ± 0.8 (-0.70^{ns})	-3.8 ± 0.6 (-15.28^{***})	0.8 ± 0.6 (2.21^{ns})	-3.1 ± 0.3 (-21.03^{**})
$Glu^{N,T}$	-0.3 ± 0.6 (-1.10^{ns})	-3.4 ± 0.5 (-16.26^{***})	-0.2 ± 0.5 (-0.90^{ns})	-3.4 ± 0.5 (-15.50^{***})	0.7 ± 0.5 (2.16^{ns})	-3.4 ± 0.2 (-37.02^{***})
$Gly^{N,?}$	-0.3 ± 0.4 (-1.56^{ns})	0.7 ± 0.3 (5.35^{ns})	0.2 ± 0.5 (1.10^{ns})	1.3 ± 0.3 (9.79^{***})	0.9 ± 0.5 (3.41^{ns})	0.8 ± 0.3 (4.79^{*})
$Ile^{E,T}$	0.1 ± 0.6 (0.39^{ns})	-2.3 ± 0.3 (-15.02^{***})	0.2 ± 0.8 (0.59^{ns})	-3.6 ± 0.4 (-21.26^{***})	0.2 ± 0.2 (2.05^{ns})	-3.3 ± 0.3 (-16.70^{**})
$Leu^{E,T}$	0.3 ± 0.6 (1.06^{ns})	-2.9 ± 0.6 (-11.39^{***})	-0.2 ± 0.3 (-1.84^{ns})	-3.8 ± 0.7 (-12.26^{***})	-0.3 ± 0.5 (-1.08^{ns})	-3.4 ± 0.2 (-26.40^{**})
$Lys^{E,S}$	na	0.3 ± 0.6 (1.05^{ns})	na	0.3 ± 0.4 (1.89^{ns})	na	0.2 ± 0.2 (1.77^{ns})
$Met^{E,S}$	na	0.1 ± 0.6 (0.54^{ns})	na	na	na	na
$Phe^{E,S}$	-0.2 ± 0.6 (-0.90^{ns})	-0.1 ± 0.3 (-0.42^{ns})	0.2 ± 0.5 (0.72^{ns})	-0.2 ± 0.2 (-2.36^{ns})	0.5 ± 0.8 (1.05^{ns})	-0.0 ± 0.4 (0.16^{ns})
$Pro^{N,T}$	-1.0 ± 0.7 (-3.03^{*})	-2.9 ± 0.5 (-13.89^{***})	-0.0 ± 0.5 (0.08^{ns})	-3.9 ± 0.2 (-37.02^{***})	0.3 ± 1.2 (0.47^{ns})	-3.3 ± 0.3 (-20.09^{**})
$Ser^{N,?}$	-0.0 ± 0.8 (0.02^{ns})	0.4 ± 0.7 (1.39^{ns})	-0.0 ± 0.7 (-0.13^{ns})	0.7 ± 0.3 (4.62^{**})	0.6 ± 1.0 (1.02^{ns})	0.3 ± 0.4 (1.33^{ns})
$Thr^{E,?}$	-0.5 ± 0.7 (-1.65^{ns})	3.4 ± 0.5 (16.72^{***})	0.3 ± 0.4 (1.97^{ns})	2.5 ± 0.6 (9.83^{***})	0.6 ± 0.3 (2.85^{ns})	2.4 ± 0.3 (15.33^{**})
$Val^{E,T}$	0.2 ± 0.6 (0.63^{ns})	-1.9 ± 0.4 (-10.45^{***})	0.2 ± 0.4 (0.87^{ns})	-2.2 ± 0.7 (-7.13^{**})	-0.8 ± 0.9 (-1.64^{ns})	-2.3 ± 0.3 (-14.53^{**})

(one sample *t*-test, $t_4 = -14.1$, $p = 1.5e^{-4}$), and *Kulamanamana* = -0.5 ± 0.1 (one sample *t*-test, $t_2 = -11.1$, $p = 0.008$).

4. DISCUSSION

Overall, the AA $\delta^{13}C$ and $\delta^{15}N$ offsets between coral polyp tissue and skeleton were consistent across three proteinaceous deep-sea coral genera. We found minimal offsets in the $\delta^{13}C$ values of both essential and non-essential AAs, as well as the $\delta^{15}N$ values of source AAs between polyp tissue and protein skeleton. However, the $\delta^{15}N$ values of trophic AAs in skeletal material were consistently 3-4‰ less than polyp tissue for all three genera. These observations suggest that these patterns of $\delta^{13}C$ and $\delta^{15}N$ offset between coral polyp tissue and proteinaceous skeleton are likely robust for gorgonin-based proteinaceous corals, linked to fundamental aspects of central metabolism and tissue synthesis. Our observations open the door for applying many of the rapidly evolving CSI-AA based tools developed for metabolically active tissues in modern systems to archival coral tissues in a paleoceanographic context.

4.1. Carbon isotopes

Amino acid carbon isotope fingerprinting has the potential to be used to reconstruct the main sources of primary production fueling consumers (e.g., Larsen et al., 2013; Arthur et al., 2014; McMahon et al., 2016). However, to apply this technique to paleoarchives, the $\delta^{13}C$ values of individual AAs in archival structural tissues, such as proteinaceous skeletons, must accurately reflect the $\delta^{13}C$ values of those same AAs in the metabolically active tissue. Our data showed only small, non-systematic offsets in AA $\delta^{13}C$ values between coral polyp tissue and proteinaceous skeleton. This observation indicates that deep-sea corals do not exhibit substantially different carbon isotope fractionation of AAs during the synthesis of metabolically active tissues and structural proteins from a shared dietary AA pool. As a result, we conclude that information obtained from the $\delta^{13}C$ values of AAs in a proteinaceous coral skeleton reflects the same information that would be obtained from the metabolically active tissue. While the average offset in AA $\delta^{13}C$ value between tissues (averaged across all AAs) was close to 0‰, there was notable variation about that mean $\delta^{13}C$ offset of individual AAs (typically <1‰) (Table 1). This variability likely reflects a combination of analytical uncertainty, small offsets in the temporal window represented by the different integration times of polyp and skeleton tissues, and potentially small differences in isotope fractionation during metabolism. However, as noted in Section 2.2.2, our best estimate of the full intra-sample variability for average $\delta^{13}C$ AA measurements using this protocol is ±0.7‰. As such, differences in AA $\delta^{13}C$ values among samples likely cannot be reliably interpreted near or less than 0.7‰.

To our knowledge, there is only one prior study comparing AA $\delta^{13}C$ values in paired metabolically active and bioarchival structural tissues (McMahon et al., 2011). In that study, McMahon et al. (2011) found minimal offsets

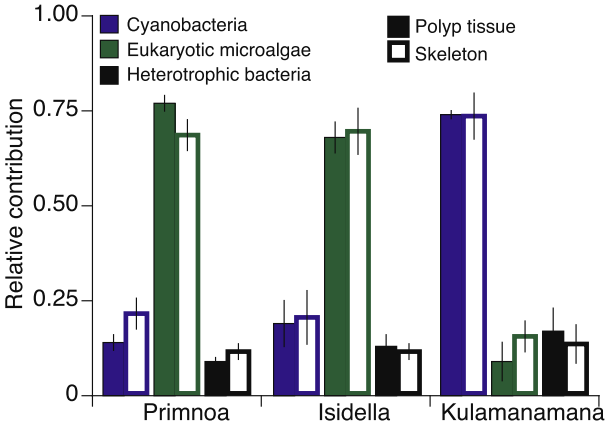

Fig. 5. Comparison of amino acid $\delta^{13}C$ fingerprinting estimates of exported plankton composition. Relative contribution of carbon from prokaryotic cyanobacteria (dark blue), eukaryotic microalgae (green), and heterotrophic bacteria (black) to three genera of proteinaceous deep-sea coral: *Primnoa pacifica* ($n = 5$), *Isidella* sp. ($n = 5$), and *Kulamanamana haumeaae* ($n = 3$) as calculated from polyp tissue (filled bars) and proteinaceous skeleton (open bars). Relative contributions were calculated using an amino acid fingerprinting approach in a fully Bayesian stable isotope mixing model framework using the normalized $\delta^{13}C$ values of five essential amino acids (Thr, Ile, Val, Phe, Leu) from published plankton end-members and deep-sea coral tissues. (For interpretation of the references to color in this figure legend, the reader is referred to the web version of this article.)

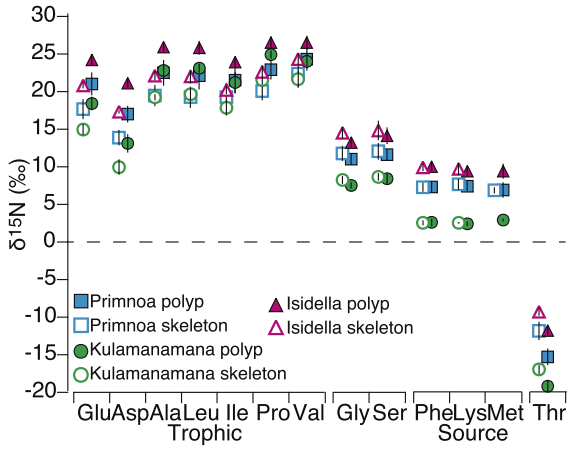

Fig. 6. Coral amino acid $\delta^{15}N$ values. Mean individual amino acid $\delta^{15}N$ values (‰ ±SD) in polyp tissue (filled symbols) and proteinaceous skeleton (open symbols) from three genera of proteinaceous deep-sea coral: *Primnoa pacifica* (cyan squares, $n = 5$), *Isidella* sp. (magenta triangles, $n = 5$), and *Kulamanamana haumeaae* (green circles, $n = 3$). (For interpretation of the references to color in this figure legend, the reader is referred to the web version of this article.)

in AA $\delta^{13}C$ values between fish muscle and the protein in biomineralized otoliths, which they similarly attributed to utilization of a shared AA pool for biosynthesis of both tissue types. Taken together, our data suggest that the AA $\delta^{13}C$ values preserved in biomineralized tissues provide a

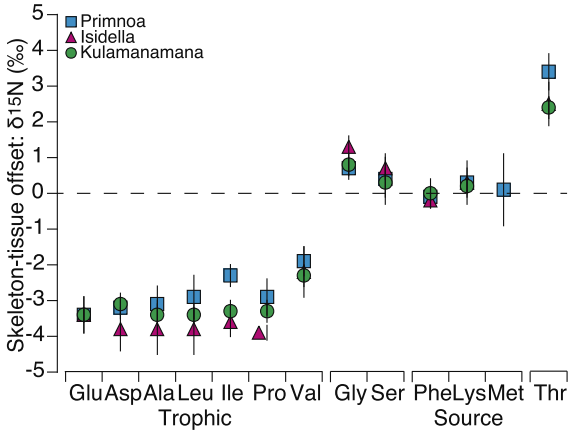

Fig. 7. Coral amino acid $\delta^{15}N$ offsets between tissues. Mean (‰ ± SD) individual amino acid $\delta^{15}N$ offset (proteinaceous skeleton minus polyp tissue) from three genera of proteinaceous deep-sea coral: *Primnoa pacifica* (cyan squares, $n = 5$), *Isidella* sp. (magenta triangles, $n = 5$), and *Kulamanamana haumeaae* (green circles, $n = 3$). (For interpretation of the references to color in this figure legend, the reader is referred to the web version of this article.)

faithful record of the AA $\delta^{13}C$ values of metabolically active tissues across phylogenetically distant consumer taxa. However, it is important to remember that given the differences in incorporation rates between coral polyps (relatively fast) and proteinaceous skeleton (skeleton), corals that experience strong seasonal changes in food source (sinking POM) could exhibit offsets in the geochemical signals recorded in these two tissues.

One promising paleo-application for proteinaceous coral skeletons is using essential AA $\delta^{13}C$ values within Bayesian mixing models to reconstruct past changes in algal community composition supporting export production (e.g., Schiff et al., 2014; McMahon et al., 2015a). The central observation for our study's main question was that both living tissue (polyp) and coral skeleton give identical (within error) estimates of plankton community composition using this technique (Fig. 5). This supports our original hypothesis that $\delta^{13}C$ AA fingerprinting approaches applied to coral skeletons produce the same result as if those analyses were conducted on metabolically active tissue integrating over the same time period.

While not the main focus of our study, our mixing model results of relative contribution of prokaryotic cyanobacteria and eukaryotic microalgae fueling export production were consistent with expectations based on phytoplankton community composition in the three oceanographically distinct regions (Fig. 5). For example, both *Primnoa* from the Gulf of Alaska and *Isidella* from the California Margin (77 ± 2% and 68 ± 4% respectively) relied heavily on export production fueled by eukaryotic microalgae, as expected for these regions with strong seasonal upwelling dominated by large eukaryotic phytoplankton (Chavez et al., 1991; Lehman, 1996; Odate, 1996; Strom et al., 2006). Conversely, *Kulamanamana* received the majority of their essential AAs from cyanobacteria-fixed carbon (74 ± 1%), consistent with the cyanobacteria-

dominated plankton composition of the oligotrophic NPSG euphotic zone (Karl et al., 2001). Our Bayesian mixing model results suggest that very little of the exported POM fed upon by any of these proteinaceous deep-sea corals was derived from heterotrophic bacteria, consistent with past estimates of direct heterotrophic bacterial contribution to sinking POM (Fuhrman, 1992; Azam et al., 1994; Wakeham, 1995). Caution must be taken when interpreting small differences (<10%) in relative contribution of end members, given the observed variability in AA $\delta^{13}C$ offsets between polyp and skeleton (Table 1), variability in the molecular isotopic training set (Table C.6), and variance in the mixing model output (±8%). As such, the fact that the relative contribution results were consistent between polyp tissue and protein skeleton within estimates of uncertainty supports our hypothesis that the proteinaceous skeletons of deep-sea corals faithfully record the same geochemical signals as metabolically active tissue over the same integration time.

4.2. Nitrogen isotopes

4.2.1. Source AA $\delta^{15}N$ as a proxy for $\delta^{15}N_{baseline}$

As we hypothesized, we found no significant offsets in source AA $\delta^{15}N$ values between proteinaceous skeleton and polyp tissue for any of the coral genera in this study (Table 1). Since source AA $\delta^{15}N$ values provide a robust proxy for $\delta^{15}N_{baseline}$ (reviewed in McMahon and McCarthy, 2016), these results provide strong validation for using source AA $\delta^{15}N$ values in proteinaceous coral records to infer past changes in the sources and cycling of nitrogen fueling export production (e.g. Sherwood et al., 2011, 2014). For instance, we found significant differences in the $\delta^{15}N_{Phe}$ values among the three coral genera from oceanographically distinct regions (Fig. 6), which were generally consistent with oceanographic regime. *Kulamanamana* corals from the NPSG had the lowest source AA $\delta^{15}N$ values (2.6 ± 0.2‰), consistent with the expected strong influence of ^{15}N-deplete nitrogen fixation in this region (Sherwood et al., 2014). Conversely, *Primnoa* from the Gulf of Alaska ($\delta^{15}N_{Phe} = 7.3 \pm 0.6$‰) and *Isidella* from the California Margin ($\delta^{15}N_{Phe} = 10.0 \pm 0.6$‰) had more enriched $\delta^{15}N_{Phe}$ values, again consistent with the nitrate supporting these coastal eutrophic upwelling systems (Wu et al., 1997; Altabet et al., 1999; Voss et al., 2001; Collins et al., 2003). *Isidella*, in particular, had the highest source AA $\delta^{15}N$ values among the specimens. This likely reflects upwelling of ^{15}N-enriched nitrate transported from regions of strong denitrification in the Eastern Tropical North Pacific via the California Undercurrent (Vokhshoori and McCarthy, 2014; Ruiz-Cooley et al., 2014).

4.2.2. Trophic AAs and $TP_{CSI\text{-}AA}$

Being able to estimate accurate $TP_{CSI\text{-}AA}$ values in bioarchives is central to many CSI-AA paleoceanographic applications. $TP_{CSI\text{-}AA}$ has been developed in coral records and sediments as a new proxy for tracking the trophic structure of planktonic ecosystems, which is likely tightly linked to overall nitrogen supply and nitricline depth (e.g., Sherwood et al., 2014; Batista et al., 2014). Measuring $TP_{CSI\text{-}AA}$ in a paleorecord is also critical to determine the degree to which shifts in $\delta^{15}N$ values of exported POM over time are driven by shifts in planktonic ecosystem structure or "baseline" changes in the sources and cycling of nitrogen at the base of the food web (e.g. Batista et al., 2014).

We found a mean 3–4‰ offset in trophic AA $\delta^{15}N$ values between skeleton and polyp tissue (Fig. 7), which was in direct contrast to both our hypothesis and the widespread assumption of consistent trophic fractionation of AAs among tissues (McMahon and McCarthy, 2016). Given the minimal offset in source AA $\delta^{15}N$ values between tissues, the estimated trophic position ($TP_{CSI\text{-}AA}$) of proteinaceous deep-sea coral from skeleton was approximately half a trophic level lower than when $TP_{CSI\text{-}AA}$ was calculated from corresponding polyp tissue. The specific $TP_{CSI\text{-}AA}$ values calculated from coral skeleton using Eq. (1) (mean 2.0 ± 0.1 across all three genera) also appear to be low based on expectations of POM feeding proteinaceous deep-sea corals. Direct $TP_{CSI\text{-}AA}$ estimates from sinking POM, for example, have generally indicated average TP values near 1.5 (e.g., McCarthy et al., 2007; Batista et al., 2014), leading to a general expectation that coral $TP_{CSI\text{-}AA}$ values should be near 2.5.

Our data indicate that a new correction factor (∂) is required for $TP_{CSI\text{-}AA}$ reconstructions from proteinaceous deep-sea coral skeletons, reflecting the observed offset in trophic AA $\delta^{15}N$ values between proteinaceous skeleton and polyp tissue. We propose a new $TP_{CSI\text{-}AA}$ equation for use with proteinaceous deep-sea coral skeletons:

$$TP_{CSI-AA-Skeleton} = 1 + \left[\frac{(\delta^{15}N_{Glu} + \partial) - \delta^{15}N_{Phe} - \beta}{TDF_{Glu-Phe}}\right] \quad (2)$$

which is modified from Eq. (1) by the addition of a correction factor (∂). For deep-sea corals with gorgonin protein (e.g. *Primnoa, Isidella, Kulamanamana*), we found a remarkably consistent ∂ for Glu of 3.4 ± 0.1‰, which when applied to skeleton Glu $\delta^{15}N$ values in Eq. (2), produced far more realistic $TP_{CSI\text{-}AA}$ estimates (2.5 ± 0.1). This means that prior $TP_{CSI\text{-}AA}$ values from deep-sea proteinaceous corals have likely been universally underestimated, however, it is important to note that comparisons of relative $TP_{CSI\text{-}AA}$ estimates using the same tissue type would not be affected by this correction factor.

4.2.3. Potential mechanisms for trophic AA $\delta^{15}N$ offsets

Our data bring up an important underlying mechanistic question: what is driving the consistent 3–4‰ offset in trophic AA $\delta^{15}N$ values between proteinaceous coral skeleton and metabolically active polyp tissue? The fact that we only observed $\delta^{15}N$ offsets for trophic AAs, but not source AAs (Fig. 7) suggests that the underlying mechanism is related to differential deamination/transamination during protein synthesis of these tissues. While confirming any specific mechanism is beyond the scope of our data, the ^{15}N-depletetion of trophic AAs in protein skeleton relative to metabolically active polyp tissue is most likely related to nitrogen flux from central Glutamine/Glutamate pool (in our protocols measured as Glu) during tissue synthesis.

The isotopic discrimination of AA nitrogen during metabolism is dependent on not only the number and iso-

tope effect of individual enzymatic reactions, but also on the turnover rate and associated relative flux of nitrogen through those pathways (Fig. C.1; e.g., Handley and Raven, 1992; Webb et al., 1998; Hayes, 2001; Germain et al., 2013; Ohkouchi et al., 2015). For example, rapid protein turnover in metabolically active tissues results in successive rounds of enzymatic isotope discrimination, leading to higher tissue $\delta^{15}N$ values than in slow turnover tissues (Waterlowm 1981; Hobson et al., 1993, 1996; Schwamborn et al., 2002; Schmidt et al., 2004). Therefore, we hypothesize that the high protein turnover and enhanced nitrogen flux in the metabolically active polyp tissue is likely linked to its ^{15}N-enrichment of trophic AAs compared to the slow growing, non-turnover proteinaceous skeleton (Hawkinsm 1985; Houlihanm 1991; Conceição et al., 1997). Because the exact biochemical pathways and associated isotope effects for the synthesis of polyp tissue and skeleton AAs are not known, we cannot evaluate any more specific mechanistic hypothesis. However, we suggest that understanding the relative nitrogen fluxes between the static (accretionary) skeleton and the rapidly cycling polyp tissues, which continually exchanges AA nitrogen with the central nitrogen pool, represents the most promising framework for future research.

Interestingly, Thr also showed a consistent $\delta^{15}N$ offset between skeleton and polyp tissue of a similar magnitude, but in the opposite direction, as the trophic AAs (Fig. 7). While the underlying metabolic processes leading to Thr nitrogen isotope fractionation remain unclear, multiple studies have noted a strong negative relationship between Thr and trophic AA nitrogen isotope fractionation during trophic transfer (Bradley et al., 2015; Nielsen et al., 2015; McMahon et al., 2015b; Mompeán et al., 2016). The consistent offset we observe does appear to be linked to coral metabolism, and so its ecological implications for the use of $\delta^{15}N_{Thr}$ values may be a valuable topic for further study.

Finally, we note that a temporal mismatch in the trophic structure of sinking POM reflected in the short-term polyp tissue and longer-term skeleton (as has been suggested in the literature for isotopic mismatches in bulk tissue e.g., Tieszen et al., 1983) cannot reasonably explain the observed offsets in trophic AA $\delta^{15}N$ values between tissues. The AA $\delta^{15}N$ values of metabolically active polyp tissue and archival protein skeleton should inherently reflect different temporal integration windows, given the different incorporation rates of these tissues. However, it seems extraordinarily unlikely that all corals in our study experienced the exact same shifts in trophic position, both in magnitude and direction, despite being collected from very distinct oceanographic regions (*Kulamanamana* from the NPSG, *Primnoa* from the Gulf of Alaska, and *Isidella* from the California Margin) spanning a decade of time (*Kulamanamana* in 2004 and 2007, *Primnoa* in 2010 and 2013, and *Isidella* in 2014).

5. CONCLUSIONS

We found that the $\delta^{13}C$ values of AAs as well as the $\delta^{15}N$ values of source AAs preserved in the proteinaceous skeletons of deep-sea gorgonin corals largely reflect the values recorded in the metabolically active polyp tissue. However, we did observe an unexpected but remarkably consistent $\delta^{15}N$ offset between trophic AAs in proteinaceous skeleton and metabolically active polyp tissue, which must be accounted for via a correction factor (∂) when calculating coral $TP_{CSI\text{-}AA}$ from proteinaceous skeletons. Future work will determine if the ∂ calculated in this study applies to other proteinaceous structural tissues, such as chitonous *Antipathes* and *Leiopathes* deep-sea corals, mollusk shells, and foraminifera tests, all of which can also provide valuable high temporal resolution archives of past ocean conditions (Serban et al., 1988; Katz et al., 2010; Prouty et al., 2014). Our results open the doors for applying many of the rapidly evolving CSI-AA-based tools developed for metabolically active tissues in modern systems to archival tissues in a paleoceanographic context.

ACKNOWLEDGEMENTS

We thank Peter Etnoyer for initiating the funded proposal for portions of this work and assisting in the collection of Primnoa samples in the Gulf of Alaska. We thank the following captains and crew of the following groups for boat logistics during sample collection: (1) the RV *Ka'imikai-o-Kanaloa* and the Hawaii Undersea Research Lab's Pisces IV and V, (2) the Monterey Bay Area Research Institute (MBARI) ROV Doc Ricketts, and (3) the H2000 ROV and FSV Alaska Provider through Scripps University. We thank undergraduates at Claremont McKenna (S. Barnes, D. Parks) and the University of California – Santa Cruz (J. Schiff, J. Liu) for assistance in sample preparation and Dr. E. Gier for assistance in compound-specific data analysis. Dr. Paul Koch (UCSC) provided input on hypotheses discussed in this paper. This work was supported by the NOAA National Undersea Research Program: West Coast and Polar Region (NA08OAR4300817) and the National Science Foundation (OCE 1061689 and OCE 1635527). A portion of this work was performed under the auspices of the U.S. Department of Energy by Lawrence Livermore National Laboratory under Contract DE-AC52-07NA27344.

APPENDIX A. SUPPLEMENTARY MATERIAL

Supplementary data associated with this article can be found, in the online version, at https://doi.org/10.1016/j.gca.2017.09.048.

REFERENCES

Altabet M. A., Pilskaln C., Thunell R., Pride C., Sigman D., Chavez F. and Francois R. (1999) The nitrogen isotope biogeochemistry of sinking particles from the margin of the eastern North Pacific. *Deep Sea Res. Part I* **46**, 655–679.

Andrews A. H., Cordes E. E., Mahoney M. M., Munk K., Coale K. H., Cailliet G. M. and Heifetz J. (2002) Age, growth, and radiometric age validation of a deep-sea, habitat-forming gorgonian (*Primnoa resedaeformis*) from the Gulf of Alaska. *Hydrobiologia* **471**, 101–110.

Arthur K. E., Kelez S., Larsen T., Choy C. A. and Popp B. N. (2014) Tracing the biosynthetic source of essential amino acids in marine turtles using δ13C fingerprints. *Ecology* **95**, 1285–1293.

Azam F., Smith D. C., Steward G. F. and Hagström Å. (1994) Bacteria-organic matter coupling and its significance for oceanic carbon cycling. *Microb. Ecol.* **28**, 167–179.

Barker S., Cacho I., Benway H. and Tachikawa K. (2005) Planktonic foraminiferal Mg/Ca as a proxy for past oceanic temperatures: a methodological overview and data compilation for the Last Glacial Maximum. *Quat. Sci. Rev.* **24**, 821–834.

Batista F. C., Ravelo A. C., Crusius J., Casso M. A. and McCarthy M. D. (2014) Compound specific amino acid $\delta^{15}N$ in marine sediments: a new approach for studies of the marine nitrogen cycle. *Geochim. Cosmochim. Acta* **142**, 553–569.

Bligh E. G. and Dyer W. J. (1959) A rapid method of total lipid extraction and purification. *Can. J. Biochem. Physiol.* **37**, 911–917.

Bradley C. J., Wallsgrove N. J., Choy C. A., Drazen J. C., Hetherington E. D., Hoen D. K. and Popp B. N. (2015) Trophic position estimates of marine teleosts using amino acid compound specific isotopic analysis. *Limnol. Oceanogr.* **13**, 476–493.

Braun A., Vikari A., Windisch W. and Auerswald K. (2014) Transamination governs nitrogen isotope heterogeneity of amino acids in rats. *J. Agric. Food Chem.* **62**, 8008–8013.

Bruland K. W., Rue E. L. and Smith G. J. (2001) Iron and macronutrients in California coastal upwelling regimes: implications for diatom blooms. *Limnol. Oceanogr.* **46**, 1661–1674.

Cairns S. D. (2007) Deep-water corals: an overview with special reference to diversity and distribution of deep-water scleractinian corals. *Bull. Mar. Sci.* **81**, 311–322.

Cairns S. D. and Bayer F. M. (2005) A review of the genus *Primnoa* (Octocorallia: Gorgonacea: Primnoidae), with the description of two new species. *Bull. Mar. Sci.* **77**, 225–256.

Chavez F. P., Barber R. T., Kosro P. M., Huyer A., Ramp S. R., Stanton T. P. and Rojas de Mendiola B. (1991) Horizontal transport and the distribution of nutrients in the coastal transition zone off northern California: effects on primary production, phytoplankton biomass and species composition. *J. Geophys. Res.* **96**, 14833–14848.

Chikaraishi Y., Kashiyama Y., Ogawa N. O., Kitazato H. and Ohkouchi N. (2007) Metabolic control of nitrogen isotope composition of amine acids in macroalgae and gastropods: implications for aquatic food web studies. *Mar. Ecol. Prog. Ser.* **342**, 85–90.

Chikaraishi Y., Ogawa N. O., Kashiyama Y., Takano Y., Suga H., Tomitani A., Miyashita H., Kitazato H. and Ohkouchi N. (2009) Determination of aquatic food-web structure based on compound-specific nitrogen isotopic composition of amino acids. *Limnol. Oceanogr.* **7**, 740–750.

Chikaraishi Y., Ogawa N. O. and Ohkouchi N. (2010) Further evaluation of the trophic level estimation based on nitrogen isotopic composition of amino acids. In *Earth, Life, and Isotopes* (eds. N. Ohkouchi, I. Tayasu and K. Koba). Kyoto University Press, Kyoto, pp. 37–51.

Chikaraishi Y., Steffan S. A., Ogawa N. O., Ishikawa N. F., Sasaki Y., Tsuchiya M. and Ohkouchi N. (2014) High-resolution food webs based on nitrogen isotopic composition of amino acids. *Ecol. Evolut.* **4**, 2423–2449.

Childers A. R., Whitledge T. E. and Stockwell D. A. (2005) Seasonal and interannual variability in the distribution of nutrients and chlorophyll a across the Gulf of Alaska shelf: 1998–2000. *Deep Sea Res. Part II* **52**, 193–216.

Church M. J., Mahaffey C., Letelier R. M., Lukas R., Zehr J. P. and Karl D. M. (2009) Physical forcing of nitrogen fixation and diazotroph community structure in the North Pacific subtropical gyre. *Global Biogeochem. Cycles* **23**.

Collins C. A., Pennington J. T., Castro C. G., Rago T. A. and Chavez F. P. (2003) The California Current system off Monterey, California: physical and biological coupling. *Deep Sea Res. Part II* **50**, 2389–2404.

Conceição L. E. C., Van der Meeren T., Verreth J. A. J., Evjen M. S., Houlihan D. F. and Fyhn H. J. (1997) Amino acid metabolism and protein turnover in larval turbot (*Scophthalmus maximus*) fed natural zooplankton or Artemia. *Mar. Biol.* **129**, 255–265.

Décima M., Landry M. R. and Popp B. N. (2013) Environmental perturbation effects on baseline δ15N values and zooplankton trophic flexibility in the southern California Current Ecosystem. *Limnol. Oceanogr.* **58**, 624–634.

Druffel E. R. M. (1997) Geochemistry of corals: proxies of past ocean chemistry, ocean circulation, and climate. *Proc. Natl. Acad. Sci.* **94**, 8354–8361.

Ehrlich H. (2010) *Biological Materials of Marine Origin*. Springer, New York.

Eppley R. W., Sharp J. H., Renger E. H., Perry M. J. and Harrison W. G. (1977) Nitrogen assimilation by phytoplankton and other microorganisms in the surface waters of the central North Pacific. *Oceanogr. Mar. Biol.* **39**, 111–120.

Fuhrman J. (1992) Bacterioplankton roles in cycling of organic matter: the microbial food web. In *Primary Productivity and Biogeochemical Cycles in the Sea* (eds. P. G. Falkowski, A. D. Woodhead and K. Vivirito). Springer, New York, pp. 361–383.

García-Reyes M. and Largier J. L. (2012) Seasonality of coastal upwelling off central and northern California: new insights, including temporal and spatial variability. *J. Geophys. Res. Ocean.* **117**, 1–17.

Germain L. R., Koch P. L., Harvey J. and McCarthy M. D. (2013) Nitrogen isotope fractionation in amino acids from harbor seals: implications for compound-specific trophic position calculations. *Mar. Ecol. Prog. Ser.* **482**, 265–277.

Goldberg W. M. (1974) Evidence of a sclerotized collagen from the skeleton of a gorgonian coral. *Comp. Biochem. Physiol. Part B* **49**, 525–526.

Gordon H. R. and Morel A. (1983) Remote assessment of ocean color for interpretation of satellite visible imagery: a review. *Lect. Notes Coast. Estaur. Study* **4**, 1–114.

Gray D. (1857) Synopsis of the families and genera of axiferous zoophytes or barked corals. *Proc. Zool. Soc. London* **25**(1), 278–294.

Guilderson T. P., McCarthy M. D., Dunbar R. B., Englebrecht A. and Roark E. B. (2013) Late Holocene variations in Pacific surface circulation and biogeochemistry inferred from proteinaceous deep-sea corals. *Biogeosciences* **10**, 6019–6028.

Hamoutene D., Puestow T., Miller-Banoub J. and Wareham V. (2008) Main lipid classes in some species of deep-sea corals in the Newfoundland and Labrador region (Northwest Atlantic Ocean). *Coral Reefs* **27**, 237–246.

Handley L. L. and Raven J. A. (1992) The use of natural abundance of nitrogen isotopes in plant physiology and ecology. *Plant, Cell Environ.* **15**, 965–985.

Hare E. P., Fogel M. L., Stafford T. W., Mitchell A. D. and Hoering T. C. (1991) The isotopic composition of carbon and nitrogen in individual amino acids isolated from modern and fossil proteins. *J. Archaeol. Sci.* **18**, 277–292.

Hawkins A. J. S. (1985) Relationships between the synthesis and breakdown of protein, dietary absorption and turnovers of nitrogen and carbon in the blue mussel, *Mytilus edulis* L. *Oecologia* **66**, 42–49.

Hayes J. M. (2001) Fractionation of carbon and hydrogen isotopes in biosynthetic processes. *Rev. Mineral. Geochem.* **43**, 225–277.

Hebert C. E., Popp B. N., Fernie K. J., Ka'apu-Lyons C., Rattner B. A. and Wallsgrove N. (2016) Amino acid specific stable nitrogen isotope values in avian tissues: insights from captive American kestrels and wild herring gulls. *Environ. Sci. Technol.* **50**, 12928–12937.

Heikoop J. M., Hickmott D. D., Risk M. J., Shearer C. K. and Atudorei V. (2002) Potential climate signals from the deep-sea gorgonian coral *Primnoa resedaeformis*. *Hydrobiologia* **471**, 117–124.

Henderson G. M. (2002) New oceanic proxies for paleoclimate. *Earth Planet. Sci. Lett.* **203**, 1–13.

Hill T. M., Myrvold C. R., Spero H. J. and Guilderson T. P. (2014) Evidence for benthic-pelagic food web coupling and carbon export from California margin bamboo coral archives. *Biogeosciences* **11**, 3845–3854.

Hobson K. A., Alisauskas R. T. and Clark R. G. (1993) Stable-nitrogen isotope enrichment in avian tissues due to fasting and nutritional stress: implications for isotopic analyses of diet. *Condor*, 388–394.

Hobson K. A., Schell D. M., Renouf D. and Noseworthy E. (1996) Stable carbon and nitrogen isotopic fractionation between diet and tissues of captive seals: implications for dietary reconstructions involving marine mammals. *Can. J. Fish. Aquat. Sci.* **53**, 528–533.

Houlihan D. F. (1991) Protein turnover in ectotherms and its relationships to energetics. In *Advances in Comparative and Environmental Physiology*. Springer, Berlin Heidelberg, pp. 1–43.

Howland M. R., Corr L. T., Young S. M. M., Jones V., Jim S., Van Der Merwe N. J., Mitchell A. D. and Evershed R. P. (2003) Expression of the dietary isotope signal in the compound-specific δ13C values of pig bone lipids and amino acids. *Int. J. Osteoarchaeol.* **13**, 54–65.

Hutchins D. A. and Bruland K. W. (1998) Iron-limited diatom growth and Si: N uptake ratios in a coastal upwelling regime. *Nature* **393**, 561–564.

Karl D. M., Bidigare R. R. and Letelier R. M. (2001) Long-term changes in plankton community structure and productivity in the North Pacific Subtropical Gyre: the domain shift hypothesis. *Deep Sea Res. Part II* **48**, 1449–1470.

Karl D. M., Bidigare R. R., Church M. J., Dore J. E., Letelier R. M., Mahaffey C. and Zehr J. P. (2008) The nitrogen cycle in the North Pacific trades biome: an evolving paradigm. *Nitro. Mar. Environ.* **2**, 705–769.

Katz M. E., Cramer B. S., Franzese A., Honisch B., Miller K. G., Rosenthal Y. and Wright J. D. (2010) Traditional and emerging geochemical proxies in foraminifera. *J. Foraminifer. Res.* **40**, 165–192.

Ladd C., Stabeno P. and Cokelet E. D. (2005) A note on cross-shelf exchange in the northern Gulf of Alaska. *Deep Sea Res. Part II* **52**, 667–679.

Larsen T., Taylor D. L., Leigh M. B. and O'Brien D. M. (2009) Stable isotope fingerprinting: a novel method for identifying plant, fungal, or bacterial origins of amino acids. *Ecology* **90**, 3526–3535.

Larsen T., Ventura M., Andersen N., O'Brien D. M., Piatkowski U. and McCarthy M. D. (2013) Tracing carbon sources through aquatic and terrestrial food webs using amino acid stable isotope fingerprinting. *PLoS ONE* **8**, e73441.

Larsen T., Bach L. T., Salvatteci R., Wang Y. V., Andersen N., Ventura M. and McCarthy M. D. (2015) Assessing the potential of amino acid patterns as a carbon source tracer in marine sediments: effects of algal growth conditions and sedimentary diagenesis. *Biogeosciences* **12**, 4979–4992.

Lehman, J., 2009. Compound-specific amino acid isotopes as tracers of algal central metabolism: developing new tools for tracing prokaryotic vs. eukaryotic primary production and organic nitrogen in the ocean. MS Thesis. University of California, Santa Cruz.

Lehman P. W. (1996) Changes in chlorophyll a concentration and phytoplankton community composition with water-year type in the upper San Francisco Bay Estuary. *San Francisco Bay: Ecosyst. Pac. Div. Am. Assoc. Adv. Sci.* **1**, 351–374.

Lehmann M. F., Bernasconi S. M., Barbieri A. and McKenzie J. A. (2002) Preservation of organic matter and alteration of its carbon and nitrogen isotope composition during simulated and in situ early sedimentary diagenesis. *Geochim. Cosmochim. Acta* **66**, 3573–3584.

Lorrain A., Graham B. S., Popp B. N., Allain V., Olson R. J., Hunt B. P., Fry B., Galván-Magaña F., Menkes C. E. R., Kaehler S. and Ménard F. (2015) Nitrogen isotopic baselines and implications for estimating foraging habitat and trophic position of yellowfin tuna in the Indian and Pacific Oceans. *Deep Sea Res. Part II* **113**, 188–198.

McCarthy M. D., Benner R., Lee C. and Fogel M. L. (2007) Amino acid nitrogen isotopic fractionation patterns as indicators of heterotrophy in plankton, particulate, and dissolved organic matter. *Geochim. Cosmochim. Acta* **71**, 4727–4744.

McClelland J. and Montoya J. (2002) Trophic relationships and the nitrogen isotopic composition of amino acids in plankton. *Ecology* **83**, 2173–2180.

McMahon K. W. and McCarthy M. D. (2016) Embracing variability in amino acid $\delta^{15}N$ fractionation: mechanisms, implications, and applications for trophic ecology. *Ecosphere* **7**, 1–26.

McMahon K. W., Fogel M. L., Elsdon T. S. and Thorrold S. R. (2010) Carbon isotope fractionation of amino acids in fish muscle reflects biosynthesis and isotopic routing from dietary protein. *J. Anim. Ecol.* **79**, 1132–1141.

McMahon K. W., Berumen M. L., Mateo I., Elsdon T. S. and Thorrold S. R. (2011) Carbon isotopes in otolith amino acids identify residency of juvenile snapper (Family: Lutjanidae) in coastal nurseries. *Coral Reefs* **30**, 1135–1145.

McMahon K. W., McCarthy M. D., Sherwood O. A., Larsen T. and Guilderson T. P. (2015a) Millennial-scale plankton regime shifts in the subtropical North Pacific Ocean. *Science* **350**, 1530–1533.

McMahon K. W., Thorrold S. R., Elsdon T. S. and McCarthy M. D. (2015b) Trophic discrimination of nitrogen stable isotopes in amino acids varies with diet quality in a marine fish. *Limnol. Oceanogr.* **60**, 1076–1087.

McMahon K. W., Thorrold S. R., Houghton L. A. and Berumen M. L. (2016) Tracing carbon flow through coral reef food webs using a compound-specific stable isotope approach. *Oecologia* **180**, 809–821.

Meyers P. A. (1994) Preservation of elemental and isotopic source identification of sedimentary organic matter. *Chem. Geol.* **114**, 289–302.

Mompeán C., Bode A., Gier E. and McCarthy M. D. (2016) Bulk vs. amino acid stable nitrogen isotope estimations of metabolic status and contributions of nitrogen fixation to size-fractionated zooplankton biomass in the subtropical North Atlantic. *Deep Sea Res. Part I* **114**, 137–148.

Nielsen J. M. and Winder M. (2015) Seasonal dynamics of zooplankton resource use revealed by carbon amino acid stable isotope values. *Mar. Ecol. Prog. Ser.* **531**, 143–154.

Nielsen J. M., Popp B. N. and Winder M. (2015) Meta-analysis of amino acid stable nitrogen isotope ratios for estimating trophic position in marine organisms. *Oecologia* **178**, 631–642.

Odate T. (1996) Abundance and size composition of the summer phytoplankton communities in the western North Pacific Ocean, the Bering Sea, and the Gulf of Alaska. *J. Oceanogr.* **52**, 335–351.

Ohkouchi N., Chikaraishi Y., Close H. G., Fry B., Larsen T., Madigan D. J., McCarthy M. D., McMahon K. W., Nagata T., Naito Y. I., Ogawa N. O., Popp B. N., Steffan S., Takano Y., Tayasu I., Wyatt A. S. J., Yamaguchi Y. T. and Yokoyama Y. (2017) Advances in the application of amino acid nitrogen

isotopic analysis in ecological and biogeochemical studies. *Org. Geochem.*. https://doi.org/10.1016/j.orggeochem.2017.07.009.

Ohkouchi N., Ogawa N. O., Chikaraishi Y., Tanaka H. and Wada E. (2015) Biochemical and physiological bases for the use of carbon and nitrogen isotopes in environmental and ecological studies. *Prog. Earth Planet. Sci.* **2**, 1–17.

Orejas C., Gili J. and Arntz W. (2003) The role of the small planktonic communities in the diet of two Antarctic octocorals (*Primnoisis antarctica* and *Primnoella* sp.). *Mar. Ecol. Prog. Ser.* **250**, 105–116.

Parnell A. C., Inger R., Bearhop S. and Jackson A. L. (2010) Source partitioning using stable isotopes: coping with too much variation. *PLoS ONE* **5**, e9672.

Parrish F. A. (2015) Settlement, colonization, and succession patterns of gold coral *Kulamanamana haumeaae* in Hawaiian deep coral assemblages. *Mar. Ecol. Prog. Ser.* **533**, 135–147.

Popp B. N., Graham B. S., Olson R. J., Hannides C. C. S., Lott M. J., López-Ibarra G. A., Galván-Magaña F. and Fry B. (2007) Insight into the trophic ecology of yellowfin tuna, *Thunnus albacares*, from compound-specific nitrogen isotope analysis of proteinaceous amino acids. *Terr. Ecol.* **1**, 173–190.

Post D. M. (2002) Using stable isotopes to estimate trophic position: models, methods, and assumptions. *Ecology* **83**, 703–718.

Prouty N. G., Roark E. B., Koenig A. E., Demopoulos A. W., Batista F. C., Kocar B. D., Selby D. and Ross S. W. (2014) Deep-sea coral record of human impact on watershed quality in the Mississippi River Basin. *Global Biogeochem. Cycles* **28**, 29–43.

R Core Team (2013) *R: A Language and Environment for Statistical Computing*. R Foundation for Statistical Computing, Vienna, Austria, <http://www.R-project.org/>.

Reeds P. J. (2000) Dispensable and indispensable amino acids for humans. *J. Nutr.* **130**, 1835S–1840S.

Ribes M., Coma R. and Gili J. M. (1999) Heterogeneous feeding in benthic suspension feeders: the natural diet and grazing rate of the temperate gorgonian *Paramuricea clavata* (Cnidaria: Octocorallia) over a year cycle. *Mar. Ecol. Prog. Ser.* **183**, 125–137.

Risk M. J., Heikoop J. M., Snow M. G. and Beukens R. (2002) Lifespans and growth patterns of two deep-sea corals: *Primnoa resedaeformis* and *Desmophyllum cristagalli*. *Hydrobiologia* **471**, 125–131.

Roark E. B., Guilderson T. P., Flood-Page S., Dunbar R. B., Ingram B. L., Fallon S. J. and McCulloch M. (2005) Radiocarbon-based ages and growth rates of bamboo corals from the Gulf of Alaska. *Geophys. Res. Lett.* **32**, 1–5.

Roark E. B., Guilderson T. P., Dunbar R. B. and Ingram B. L. (2006) Radiocarbon-based ages and growth rates of Hawaiian deep-sea corals. *Mar. Ecol. Prog. Ser.* **327**, 1–14.

Roark E. B., Guilderson T. P., Dunbar R. B., Fallon S. J. and Mucciarone D. A. (2009) Extreme longevity in proteinaceous deep-sea corals. *Proc. Natl. Acad. Sci.* **106**, 5204–5208.

Roberts S. and Hirshfield M. (2004) Deep-sea corals: out of sight, but no longer out of mind. *Front. Ecol. Environ.* **2**, 123–130.

Robinson L. F., Adkins J. F., Frank N., Gagnon A. C., Prouty N. G., Brendan Roark E. and van de Flierdt T. (2014) The geochemistry of deep-sea coral skeletons: a review of vital effects and applications for palaeoceanography. *Deep Res. Part II* **99**, 184–198.

Rothwell R. G. and Rack F. R. (2006) New techniques in sediment core analysis: an introduction. *Geol. Soc. Lond. Spec. Publ.* **267**, 1–29.

Ruiz-Cooley R. I., Koch P. L., Fiedler P. C. and McCarthy M. D. (2014) Carbon and nitrogen isotopes from top predator amino acids reveal rapidly shifting ocean biochemistry in the Outer California Current. *PLoS ONE* **9**, e110355.

Sambrotto R. N. and Lorenzen C. J. (1986) Phytoplankton and primary production. In *The Gulf of Alaska: Physical Environment and Biological Resources* (eds. D. W. Hood and S. T. Zimmerman). US Department of Commerce, Washington, DC, pp. 249–282.

Schiff J. T., Batista F. C., Sherwood O. A., Guilderson T. P., Hill T. M., Ravelo A. C., McMahon K. W. and McCarthy M. D. (2014) Compound specific amino acid $\delta_{13}C$ patterns in a deep-sea proteinaceous coral: Implications for reconstructing detailed $\delta_{13}C$ records of exported primary production. *Mar. Chem.* **166**, 82–91.

Schmidt K., McClelland J. W., Mente E., Montoya J. P., Atkinson A. and Voss M. (2004) Trophic-level interpretation based on $\delta^{15}N$ values: implications of tissue-specific fractionation and amino acid composition. *Mar. Ecol. Prog. Ser.* **266**, 43–58.

Schwamborn R., Ekau W., Voss M. and Saint-Paul U. (2002) How important are mangroves as a carbon source for decapod crustacean larvae in a tropical estuary? *Mar. Ecol. Prog. Ser.* **229**, 195–205.

Scott J. H., O'Brien D. M., Emerson D., Sun H., McDonald G. D., Salgado A. and Fogel M. L. (2006) An examination of the carbon isotope effects associated with amino acid biosynthesis. *Astrobiology* **6**, 867–880.

Serban A., Engel M. H. and Macko S. A. (1988) The distribution, stereochemistry and stable isotopic composition of amino acid constituents of fossil and modern mollusk shells. *Org. Geochem.* **13**, 1123–1129.

Sherwood O. A. and Edinger E. N. (2009) Ages and growth rates of some deep-sea gorgonian and antipatharian corals of Newfoundland and Labrador. *Can. J. Fish. Aquat. Sci.* **66**, 142–152.

Sherwood O. A., Scott D. B., Risk M. J. and Guilderson T. P. (2005) Radiocarbon evidence for annual growth rings in the deep-sea octocoral *Primnoa resedaeformis*. *Mar. Ecol. Prog. Ser.* **301**, 129–134.

Sherwood O. A., Thresher R. E., Fallon S. J., Davies D. M. and Trull T. W. (2009) Multi-century time-series of ^{15}N and ^{14}C in bamboo corals from deep Tasmanian seamounts: evidence for stable oceanographic conditions. *Mar. Ecol. Prog. Ser.* **397**, 209–218.

Sherwood O. A., Lehmann M. F., Schubert C. J., Scott D. B. and McCarthy M. D. (2011) Nutrient regime shift in the western North Atlantic indicated by compound-specific $\delta^{15}N$ of deep-sea gorgonian corals. *Proc. Natl. Acad. Sci.* **108**, 1011–1015.

Sherwood O. A., Guilderson T. P., Batista F. C., Schiff J. T. and McCarthy M. D. (2014) Increasing subtropical North Pacific Ocean nitrogen fixation since the Little Ice Age. *Nature* **505**, 78–81.

Silfer J. A., Engel M. H., Macko S. A. and Jumeau E. J. (1991) Stable carbon isotope analysis of amino acid enantiomers by conventional isotope ratio mass spectrometry and combined gas chromatography/isotope ratio mass spectrometry. *Anal. Chem.* **63**, 370–374.

Sinniger F., Ocana O. V. and Baco A. R. (2013) Diversity of zoanthids (Anthozoa: Hexacorallia) on Hawaiian seamounts: description of the Hawaiian gold coral and additional zoanthids. *PLoS ONE* **8**, e52607.

Strom S. L., Olson M. B., Macri E. L. and Mordy C. W. (2006) Cross-shelf gradients in phytoplankton community structure, nutrient utilization, and growth rate in the coastal Gulf of Alaska. *Mar. Ecol. Prog. Ser.* **328**, 75–92.

Strub P. T., Allen J. S., Huyer A., Smith R. L. and Beaedsley R. C. (1987) Seasonal cycles of currents, temperatures, winds, and sea level over the northeast pacific continental shelf: 35N to 48N. *J. Geophys. Res. Ocean.* **92**, 1507–1526.

Strzepek K. M., Thresher R. E., Revill A. T., Smith C. I., Komugabe A. F. and Fallon S. F. (2014) Preservation effects on

the isotopic and elemental composition of skeletal structures in the deep-sea bamboo coral *Lepidisis* spp. (Isididae). *Deep Res. Part II* **99**, 199–206.

Thresher R., Rintoul S. R., Koslow J. A., Weidman C., Adkins J. and Proctor C. (2004) Oceanic evidence of climate change in southern Australia over the last three centuries. *Geophys. Res. Lett.* **31**, 2–5.

Tieszen L. L., Boutton T. W., Tesdahl K. G. and Slade N. A. (1983) Fractionation and turnover of stable carbon isotopes in animal tissues: implications for $\delta^{13}C$ analysis of diet. *Oecologia* **57**, 32–37.

Ueda K., Morgan S. L., Fox A., Gilbart J., Sonesson A., Larsson L. and Odham G. (1989) D-alanine as a chemical marker for the determination of streptococcal cell wall levels in mammalian tissues by gas chromatography/negative ion chemical ionization mass spectrometry. *Anal. Chem.* **61**, 265–270.

Vokhshoori N. L. and McCarthy M. D. (2014) Compound-specific $\delta^{15}N$ amino acid measurements in littoral mussels in the California upwelling ecosystem: a new approach to generating baseline $\delta^{15}N$ isoscapes for coastal ecosystems. *PLoS ONE* **9**, e98087.

Voss M., Dippner J. W. and Montoya J. P. (2001) Nitrogen isotope patterns in the oxygen-deficient waters of the Eastern Tropical North Pacific Ocean. *Deep Res. Part I* **48**, 1905–1921.

Wakeham S. G. (1995) Lipid biomarkers for heterotrophic alteration of suspended particulate organic matter in oxygenated and anoxic water columns of the ocean. *Deep Sea Res. Part I* **42**, 1749–1771.

Wakeham S. G. and Lee C. (1989) Organic geochemistry of particulate matter in the ocean: the role of particles in oceanic sedimentary cycles. *Org. Geochem.* **14**, 83–96.

Walker B. D. and McCarthy M. D. (2012) Elemental and isotopic characterization of dissolved and particulate organic matter in a unique California upwelling system: importance of size and composition in the export of labile material. *Limnol. Oceanogr.* **57**, 1757–1774.

Ward E. J., Semmens B. X. and Schindler D. E. (2010) Including source uncertainty and prior information in the analysis of stable isotope mixing models. *Environ. Sci. Technol.* **44**, 4645–4650.

Waterlow J. C. (1981) N end-product methods for the study of whole body protein turnover. *Proc. Nutr. Soc.* **40**, 317–320.

Webb S., Hedges R. and Simpson S. (1998) Diet quality influences the $\delta^{13}C$ and $\delta^{15}N$ of locusts and their biochemical components. *J. Exp. Biol.* **201**, 2903–2911.

Williams B., Risk M., Stone R., Sinclair D. and Ghaleb B. (2007) Oceanographic changes in the North Pacific Ocean over the past century recorded in deep-water gorgonian corals. *Mar. Ecol. Prog. Ser.* **335**, 85–94.

Williams B., Thibodeau B., Chikaraishi Y., Ohkouchi N., Walnum A., Grottoli A. and Colin P. (2016) Consistency in coral skeletal amino acid composition offshore of Palau in the western Pacific warm pool indicates no impact of decadal variability in nitricline depth on primary productivity. *Limnol. Oceanogr.* **62**, 399–407.

Wu J., Calvert S. E. and Wong C. S. (1997) Nitrogen isotope variations in the subarctic northeast Pacific: relationships to nitrate utilization and trophic structure. *Deep Res. Part I* **44**, 287–314.

Associate editor: Ruth Blake